RESEARCH

Experimental and MCFT-Based Study on Steel Fiber-Reinforced Concrete Subjected to In-Plane Shear Forces

Suyash K. Wagh, Agie Vianthi and Wen-Cheng Liao[*]

Abstract

Testing of concrete panels subjected to pure in-plane shear loading is necessary to elucidate the shear behavior of concrete. However, available data for predicting the shear capacity and behavior of steel fiber-reinforced concrete are rather limited. This study aims to evaluate the shear capacity and behavior of fiber-reinforced concrete made of highly flowable strain hardening fiber-reinforced concrete (HF-SHFRC) experimentally and analytically, respectively, using a panel tester loaded under pure shear and modified compression field theory (MCFT). The test was conducted using a panel test machine at the University of Toronto. The test results of the HF-SHFRC demonstrated strain hardening behavior at tension after the first crack, as indicated by the increase in the shear stress after the first crack in the HF-SHFRC panel. An analysis procedure is proposed for predicting the shear strength of steel fiber-reinforced concrete (SFRC) based on experimental data of the SFRC panels to obtain reliable results. A comparison of results obtained from the proposed analysis procedure and experiments show that it accurately predicted the response of the HF-SHFRC. The proposed MCFT-based analysis procedure can provide valuable insight for understanding the behavior of the SFRC panels under shear loading.

Keywords Steel fiber, Reinforced concrete, Panels, In-plane shear, Modified compression field theory, Shear behavior

1 Introduction

Steel fiber-reinforced concrete (SFRC), as a composite material, exhibits excellent properties, such as tensile, flexural, and shear strengths, crack resistance, and toughness (Kwak et al., 2002; Susetyo et al., 2011). Currently, SFRC is commonly used in the construction of beam elements, tunnel linings, and road pavements. Because of its brittle nature, concrete can collapse suddenly without prior warning shortly after the formation of the first crack when the principal tensile

stress exceeds the tensile strength of the concrete within the shear span of the reinforced concrete (RC) element (Narayanan & Darwish, 1987). The addition of fibers can overcome these shortcomings by improving the crack-controlling characteristics and resistance to large crack widths. Hence, an in-depth analysis of the behavior of SFRC by evaluating all factors affecting the shear strength is required.

Most studies have focused on the effect of fiber-reinforced concrete on beams to predict the shear strength (Ashour et al., 1992; Mansur et al., 1986; Narayanan & Darwish, 1987) using universally accepted conventional two-point loading tests. For fiber-reinforced concrete with a volume content of fiber (V_f) $\geq$ 0.75%, the shear stress was observed to be greater than or equal to $0.3\sqrt{f_c'}$ irrespective of the depth of the beam (d) and concrete compressive strength $\left(f_c'\right)$ (Parra-montesinos, 2006). In contrast, f_c' affects the shear strength of

*Correspondence:
Wen-Cheng Liao
wcliao@ntu.edu.tw
Department of Civil Engineering, College of Engineering, National Taiwan University, No. 1, Sec. 4, Roosevelt Road, Da'an District, Taipei 10617, Taiwan

Wagh *et al. Int J Concr Struct Mater*   (2023) 17:29

Page 2 of 13

conventional RC beams (Narayanan & Darwish, 1987). In both SFRC and conventional RC beams, the shear span–depth ratio (a/d) also affects the shear strength (Ashour et al., 1992; Mansur et al., 1986; Narayanan & Darwish, 1987; Noghabai, 2000; Parra-montesinos, 2006). Using steel fibers as an alternative for minimum transverse reinforcement, Parra-Montesinos (2006) reported that the minimum value for the volume content of steel fibers (V_f) is 0.75% based on available data on 147 SFRC beams.

Apart from the conventional experimental methods for estimating the shear strength of reinforced concrete elements subjected to shear, some tests have been conducted using the panel element testing facility at the University of Toronto and the modified compression field theory (MCFT) was proposed (Vecchio & Collins, 1986). This method is effective and widely used for shear analysis of reinforced concrete members. Moreover, the membrane element testing facility was used to assess SFRC panels to evaluate their effectiveness for minimum shear reinforcement. It was found that a volume content of 1% steel fibers is required to achieve satisfactory shear performance. Experiments conducted using a panel element tester show that the fiber aspect ratio has a significant effect on shear strength, whereas the compressive strength of concrete does not (Susetyo et al., 2011). An extension of MCFT evolved in a more refined way as a disturbed stress field model (DSFM) (Vecchio, 2000). Based on DSFM, Susetyo et. al. (2013) and Lee et. al. (2016) proposed an analysis procedure for the SFRC elements by using the finite element approach and implementing the variable engagement model (VEM) and diverse embedment model (DEM), respectively, as tension models. Over the period of 3 decades MCFT remains the versatile model for the analysis of shear response of reinforced concrete elements. At present, MCFT is considered as a basis for shear design in many design codes as well as adapted in the finite element analysis programs and recognized more over DSFM (Sadeghian & Vecchio, 2018). Consequently, it is deemed necessary to understand the applicability of MCFT for predicting the shear behavior of SFRC elements. Furthermore, the addition of fiber reduces the workability of SFRC in its fresh state, and the presence of a dense reinforcement mesh affects the flowability of concrete. This problem can be addressed using highly flowable strain hardening fiber-reinforced concrete (HF-SHFRC) with high flowability and moderate viscosity. In HF-SHFRC, low water-to-cement ratio can be maintained with appropriate addition of superplasticizers (SP) and viscosity modifying agents (VMA). Also, HF-SHFRC exhibits enhanced concrete durability, resistance to sulfate attack, and salt penetration (Liao & Su, 2018; Liao et al., 2017).

Therefore, this study focused on the response of HF-SHFRC panels subjected to in-plane shear stresses. A parametric study was conducted by comparing experimental data for HF-SHFRC panels with high-strength and normal-strength RC/SFRC panel specimen data obtained from studies by Vecchio and Collins (1986) and Susetyo (2009). In addition, MCFT was applied for predicting the stress–strain response of the SFRC panels and an analysis procedure is proposed. Finally, the proposed analysis procedure was validated using experimental results from the literature.

The scope of this paper includes the description of the experimental program for testing the HF-SHFRC panels in the panel test machine, proposed analytical model, solution method, discussion of the experimental results, discussion of the analytical results, and verification of the proposed model followed by the conclusion of this study.

2 Research Significance

HF-SHFRC has outstanding workability as well as strain hardening and improved multiple cracking characteristics in its fresh and hardened states, respectively. Therefore, its shear loading conditions should be investigated. This study provides insight into the behavior of HF-SHFRC panels subjected to monotonic pure shear loading. It is well known that the shear stress–strain response of RC panels can be accurately predicted using MCFT. However, MCFT cannot reflect the effect of steel fiber addition on concrete. This is because the tensile properties of SFRC are different from those of reinforced concrete, and the tensile model used in formulating MCFT is inadequate. In this study, an analysis procedure is proposed for predicting the shear behavior of SFRC panels with reinforcement in the longitudinal direction only based on MCFT. In addition, the analysis procedure can be used to predict the possible failure patterns of SFRC panel specimens.

3 Experimental Program

In this study, two normal-strength HF-SHFRC panels were tested based on the extensive testing program proposed by Vecchio and Collins (1986) and Susetyo (2009) on shear panels. Both panels were tested at the University of Toronto using a panel element tester under pure monotonic in-plane shear loading. Details of the panel specimens are presented in Table 1.

3.1 Materials Constitution

The mixing proportion of concrete and properties of the hooked-end steel fibers are listed in Tables 2 and 3, respectively. Two types of steel fibers, obtained from N.V. Bekaert S.A., with different geometries were used. Both types differ in length and diameter, but their aspect ratios

Wagh *et al. Int J Concr Struct Mater*   (2023) 17:29

Page 3 of 13

Table 1 Details of the panel specimens

Specimen ID	Concrete type	f'_c (MPa)	Fiber type	V_f (%)	Longitudinal steel		Transverse steel	
					ρ_{sx} (%)	f_{yx} (MPa)	ρ_{sy} (%)	f_{yy} (MPa)
HFF1V1	Normal strength	35	RC80/30-BP	1.5	2.47	552	–	–
HFF2V2		21	RC80/60-BN	0.75	2.47	552	–	–

Table 2 Concrete mix proportion

| Material	Proportion
Cement (ASTM type III)	1
Fly ash (Class C)	0.875
Fine aggregate	2.2
Coarse aggregate	1.2
Water	0.8
Superplasticizer (SP)	0.005
Viscosity modifying admixtures (VMA)	0.038

Table 3 Geometry and properties of fiber

Fiber type	l_f (mm)	d_f (mm)	Aspect ratio	Tensile strength (MPa)
RC 80/30 BP	30	0.38	79	2300
RC 80/60 BN	60	0.75	80	1050

are nearly the same. The coarse to fine aggregate ratio was adjusted to limit the reduction in workability due to the addition of fiber. It has been suggested that the coarse to

fine aggregate ratio can be reduced by fulfilling the criteria of workability and strength (Liao et al., 2006). Coarse aggregate with a maximum size of 10 mm was used. The chemical admixtures were added to ensure appropriate workability of the concrete. In addition, a comprehensive performance-based HF-SHFRC mix design methodology for target slump flow and strength based on dense packing concept was applied in this mix design procedure (Liao et al., 2017). The details of the materials and concrete mix procedure used in this study is the same as that proposed by Susetyo (2009). Batching and mixing were carried out at the facility at the University of Toronto.

3.2 Specimen description and panel test

Panel specimens with dimensions of $890 \times 890 \times 70$ mm were constructed with two layers of reinforcement in the longitudinal direction only. Shear keys, as shown in Fig. 1a, facilitate the arrangement of the reinforcement in two layers. Table 1 presents details of the reinforcement. Both panels consist of 2.47% reinforcement in the longitudinal direction only. Cold-formed deformed bars were used for the reinforcement. Contributing to the resistance in transverse direction is from steel fibers only. After assembling the reinforcing bars and shear keys, the specimen was cast

(a)

(b)
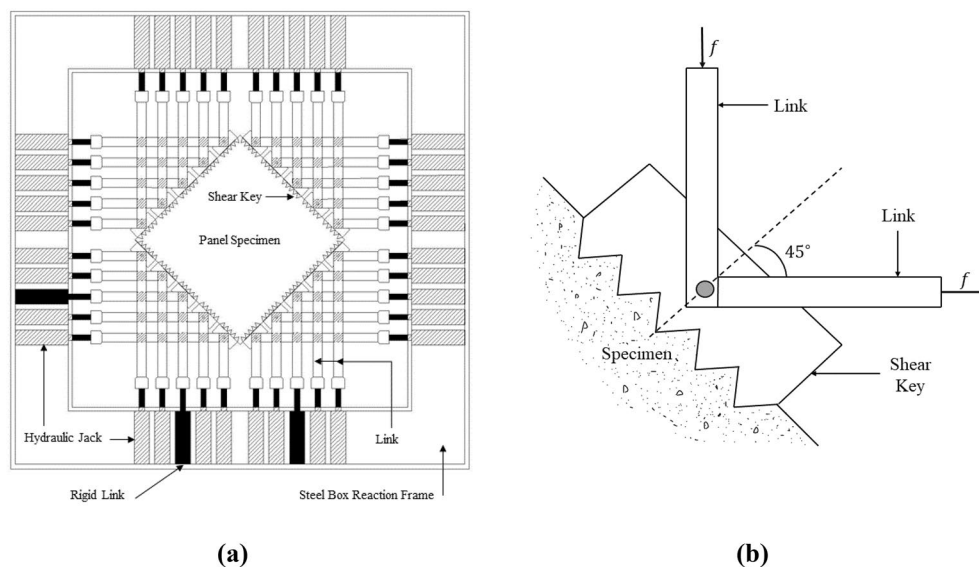
Fig. 1 **a** Diagrammatic representation of the panel element test facility; **b** link–shear key assembly

in a steel formwork. Rubber spacers were used between the gaps of the two shear keys to enclose the formwork and prevent the cement slurry from flowing out of the formwork. Twenty shear keys were cast on all four sides of the panel, with five shear keys on each side. The reinforcement was spliced with a 5/16″ threaded rod to bolt it with the shear keys. Threaded rods or shear studs were spliced into the reinforcement to facilitate load transfer from the shear key to the reinforced concrete panel. A nut-and-washer system was provided to ensure proper mechanical anchorage at the end of the threaded rod. The specimens were tested after 7 days of curing.

The tests were conducted using the panel element test facility developed by Vecchio and Collins (1986) at the University of Toronto, which can be used to apply various in-plane loads. A panel test is usually conducted for a better overall understanding of the interaction between the reinforcement and fiber-reinforced concrete, which is limited in uniaxial tensile tests (Susetyo, 2009). The components of the panel test machine are shown in Fig. 1. The panel test machine consists of a steel box reaction frame that houses the jack and link assembly, as shown in Fig. 1a. The specimens were loaded into the test facility by connecting the two links to each shear key. Both specimens were subjected to pure monotonic shear. A force was applied to the shear keys through a grid of 40 links. In the grid, 37 links (around the periphery of the member) induce the force in the shear keys using double-acting hydraulic jacks. The remaining three links act as rigid links to stabilize the panel within the test rig (Vecchio, 1982). The machine comprises a lateral support frame and tie rods to prevent out-of-plane displacement of the specimen. One

link is subjected to a compressive force, whereas the other is subjected to an equal amount of tensile force to achieve a pure shear condition in the panel, as shown in Fig. 1b. Panel should be loaded properly in the machine to avoid the out-of-plane displacement. This displacement can be the result of overtightening of the bolt connecting links to shear key (Fig. 1b) and setting up inappropriate length of the links.

Strain gauges and linear variable differential transducers (LVDTs) were fixed on the panel to constantly measure the strain in all four directions in the panel. LVDTs were installed on the front and back faces of the panel to measure the average strains in the vicinity of a certain gauge length; they do not exhibit localized strain behavior. Twelve LVDTs were fixed on the front and back sides of the panel, and their orientations are illustrated in Fig. 2a. The Zurich gauge is a mechanical strain device that exhibits localized strain behavior. In this strain measurement method, 16 aluminum targets were fixed on each face of the panel specimen. Fig. 2b depicts the layout of the aluminum targets fixed on a grid of 200×200 mm. Furthermore, the measurements from the Zurich gauge were averaged and used to validate those obtained from the LVDTs. The load was increased monotonically until failure, and the strain in the panel specimen was measured at each load stage. Strain gauges were fixed on the steel reinforcement to measure the local strain.

3.3 Parametric Study

A parametric study was conducted to determine the behavior of the HF-SHFRC panels. The analysis results of the four panels were obtained from Vecchio and Collins (1986) and Susetyo (2009) for comparison. Vecchio and Collins conducted an extensive study on shear panels
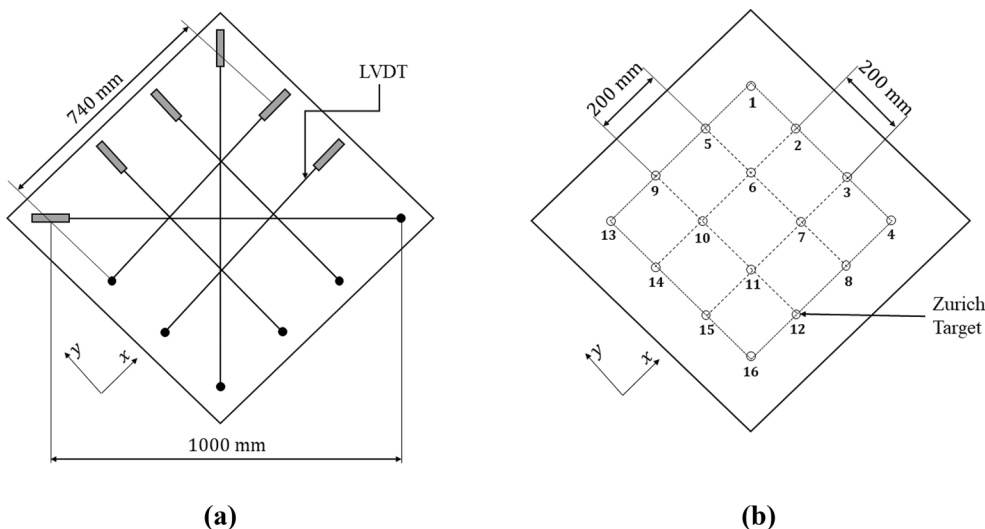

Fig. 2 **a** Arrangement of LVDTs for the panel test; **b** layout of Zurich targets

Wagh *et al. Int J Concr Struct Mater* (2023) 17:29

Page 5 of 13

under various loading conditions, concrete compressive strengths, and reinforcement ratios. Susetyo examined SFRC panels to seek the replacement for minimum shear reinforcement by varying the fiber type and content. Therefore, the test sets presented in Table 4 facilitate the comparison. Panels with both longitudinal and transverse reinforcements were used as control panels in the respective studies. The proportions of concrete mix, mixing procedures, and testing of panel specimens PV6, PV13, C2C, and C2F2V3 can be found in the studies by Vecchio (1982) and Susetyo (2009).

4 Development of Analytical Model

MCFT (Vecchio & Collins, 1986) was developed from compression field theory (Collins, 1978; Mitchell & Collins, 1974). Its development involves testing many reinforced concrete panels by applying distinct loading conditions, such as uniaxial compression, pure shear, or a combination of shear and biaxial stresses. The MCFT is formulated upon compatibility, equilibrium, and constitutive laws of materials with a primary assumption that, in concrete, the direction of principal stress corresponds with the direction of principal strain. MCFT also considers the cracked concrete as a new orthotropic material with its unique characteristics, which strongly affects the calculated response. Analysis based on MCFT consists of a step-by-step procedure for calculating the response of the loaded elements.

In this study, SFRC panel specimens subjected to shear were investigated to compare their experimental and analytical responses by applying modified compression field theory. In the proposed analysis procedure, strain hardening behavior of SFRC was taken into consideration by modifying the material constitutive laws. This principal modification along with some minor modifications depicted in consecutive sections will enable MCFT to predict the shear strength of SFRC with reinforcement in the longitudinal direction only.

4.1 Constitutive Laws of Materials
4.1.1 Constitutive Laws for Cracked Concrete
Concrete in compression: Eq. (1) is applied to determine the behavior of the cracked concrete, where the value of the strain in the concrete with respect to the peak stress (ε_c') in cylinder compression is usually taken as -0.002 (negative quantity). The average maximum principal compressive stress in the cracked concrete $(f_{c2\,max})$ can be expressed as given in Eq. (2). Both the Eqs. (1) and (2) were drawn from Vecchio and Collins (1986):

$$f_{c2} = f_{c2\,max} \left[\frac{2\varepsilon_2}{\varepsilon_c'} - \left(\frac{\varepsilon_2}{\varepsilon_c'} \right)^2 \right], \tag{1}$$

$$f_{c2\,max} = \frac{f_c'}{0.8 - 0.34 \left(\frac{\varepsilon_1}{\varepsilon_c'} \right)} \leq 1.0. \tag{2}$$

Concrete in tension: to determine the tensile behavior of SFRC, Eq. (3) provides the relationship between the principal tensile stress (f_{c1}) and strain (ε_1) in concrete prior to cracking. In addition, a model proposed by Naaman (1972) based on the statistical mechanics of composite materials was adopted to represent the ductile behavior of SFRC after cracking. Therefore, at this stage, f_{c1} can be estimated using Eq. (4).

$$f_{c1} = E_c \varepsilon_1 \text{ for } \varepsilon_1 \leq \varepsilon_{cr} \text{(ascending branch)}, \tag{3}$$

$$f_{c1} = \sigma_{cc} + \frac{\sigma_{pc} - \sigma_{cc}}{\varepsilon_{pc} - \varepsilon_{cc}} \times (\varepsilon_1 - \varepsilon_{cc}) \text{ for (strain hardening branch).} \tag{4}$$

where σ_{cc} and σ_{pc} are the first crack and post-cracking strengths of the concrete, respectively, ε_{cc} and ε_{pc} are the cracking strain and maximum strain in the concrete, respectively, and E_c is the modulus of elasticity of the concrete in MPa. These parameters are derived as follows:

Table 4 Test sets

Specimen ID	Concrete type	f_c' (MPa)	Fiber type	V_f (%)	Longitudinal steel		Transverse steel	
					ρ_{sx} (%)	f_{yx} (MPa)	ρ_{sy} (%)	f_{yy} (MPa)
Tests conducted by Vecchio and Collins								
PV6	Normal strength	29.8	–	–	1.79	266	1.79	266
PV13		18.2	–	–	1.79	248	–	–
Test conducted by Susetyo								
C2C	High strength	90.5	–	–	3.31	552	0.42	477
C2F2V3		76.5	RC80/30-BP	1.5	3.31	552	–	–

Wagh *et al. Int J Concr Struct Mater*   (2023) 17:29

Page 6 of 13

$$\sigma_{cc} = \sigma_{mu}(1 - V_f) + \alpha\tau_{eq}V_f\left(\frac{l_f}{d_f}\right), \tag{5}$$

$$\sigma_{pc} = \lambda\tau_{eq}V_f\left(\frac{l_f}{d_f}\right), \tag{6}$$

$$E_c = 4700\sqrt{f_c'}, \tag{7}$$

where the strength at the cracking of the concrete $(\sigma_{mu}) = 0.33\sqrt{f_c'}$ (MPa).

According to ACI Committee 363 (2005), concrete can be categorized as high-strength and normal-strength (low-strength) concrete. High-strength concrete exhibits compressive strength exceeding 55 MPa. The values of the equivalent bond strength at the interface of the fiber and matrix (τ_{eq}) were selected based on these two categories. For high-strength concrete, $\tau_{eq} = 5.6$ MPa and for normal-strength concrete, $\tau_{eq} = 4.65$. These average values were obtained directly from the fiber pull-out tests conducted by Liao et. al. (2015) using hooked-end steel fibers with different mix proportions. Alternatively, τ_{eq} can be estimated from the VEM, $\tau_{eq} = 0.825\sqrt{f_c'}$ MPa. However, this model can underestimate the pull-out strength of hooked-end steel fibers because it considers only the effect of frictional bond characteristics and not the mechanical anchorage (Lee et al., 2011; Voo & Foster, 2003). Moreover, α and λ are, respectively, taken as 0.25 and 0.65, which are the products of several coefficients; in this study, these values were derived from the uniaxial tension tests conducted by Susetyo (2009).

Furthermore, inserting $\varepsilon_{pc} = 0.007$ into Eq. (4) yields Eq. (8). In the direct tensile test, the maximum tensile strain is 0.7% (Chao et al., 2007; Liao et al., 2006). Antithetically, plain concrete also reaches a maximum tensile strain value of 0.7% (Evans & Marathe, 1968); hence, Eq. (8) is conservative for both plain concrete and SFRC:

$$f_{c1} = \sigma_{cc} + \frac{\sigma_{pc} - \sigma_{cc}}{0.007 - \varepsilon_{cc}} \times (\varepsilon_1 - \varepsilon_{cc}). \tag{8}$$

4.1.2 Models for Conventional Reinforcement

For bare reinforcing steel bars, the usual bilinear, elastic-perfectly plastic stress–strain relationship is assumed and can be expressed as

$$f_{sx} = E_s\varepsilon_x, \tag{9}$$

$$f_{sy} = E_s\varepsilon_y, \tag{10}$$

where E_s is the elastic modulus of steel bars, f_s and E_s are the stress and strain in steel, respectively, and ε_x and ε_y are the strain in steel in the x and y directions, respectively.

4.2 Strain Compatibility

Assuming that at any instance of loading, the strains in steel and concrete are the same ($\varepsilon_s = \varepsilon_c = \varepsilon$), Mohr's circle for strains in the ε and $\gamma/2$ coordinate system (as shown in Fig. 3) represents the geometric relationships for the three strain components from Eqs. (11) to (13).
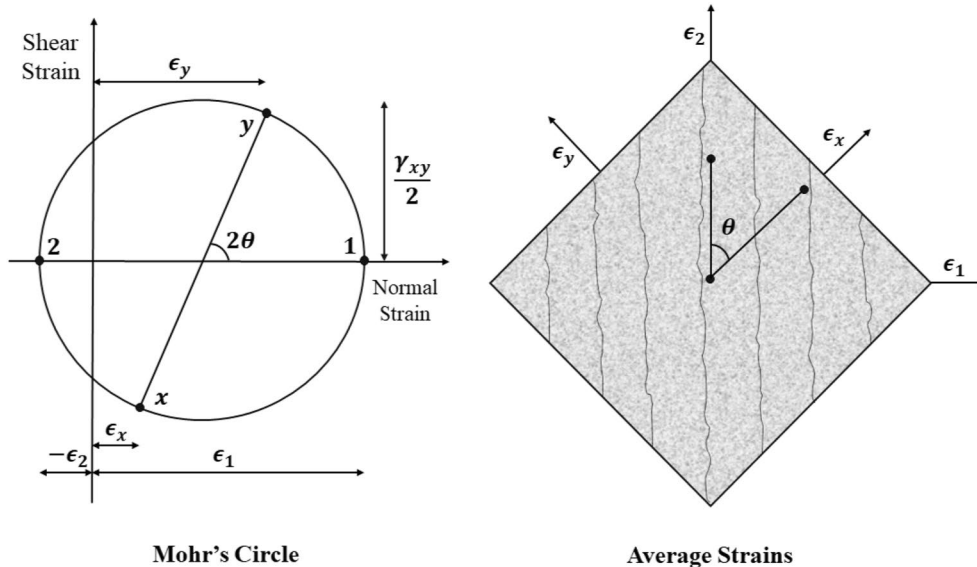

Fig. 3 Strain compatibility for cracked element

Wagh *et al. Int J Concr Struct Mater* (2023) 17:29

Page 7 of 13

$$\gamma_{xy} = 2(\varepsilon_x - \varepsilon_2)/\tan\theta, \tag{11}$$

$$\varepsilon_x = \varepsilon_1 + \varepsilon_2 - \varepsilon_y, \tag{12}$$

$$\varepsilon_y = \frac{\varepsilon_1 + \varepsilon_2 \tan^2\theta}{1 + \tan^2\theta}. \tag{13}$$

The principal compressive strain in concrete (ε_2) (negative quantity) can be numerically evaluated as follows:

$$\varepsilon_2 = \varepsilon_c'\left(1 - \sqrt{1 - \frac{f_{c2}}{f_{c2max}}}\right). \tag{14}$$

The equation for determining angle θ based on Mohr's compatibility truss model is as follows:

$$\tan^2\theta = \frac{\varepsilon_x - \varepsilon_2}{\varepsilon_y - \varepsilon_2}. \tag{15}$$

4.3 Force Equilibrium

Before cracking, the applied forces are resisted by the combined action of steel and concrete. Based on the finding presented in Vecchio and Collins (1986), the following equilibrium equations were adopted after eliminating the difference between the actual cross-sectional areas of concrete before and after incorporating the reinforcing bars. In other words, reduction in the cross-sectional area of concrete due to the presence of reinforcement was not considered.

$$f_x = f_{cx} + \rho_{sx} f_{sx}, \tag{16}$$

$$f_y = f_{cy} + \rho_{sy} f_{sy}, \tag{17}$$

$$v_{xy} = (f_{c1} - f_{cy})/\tan\theta, \tag{18}$$

$$f_{cx} = f_{c1} - \frac{v_{xy}}{\tan\theta}, \tag{19}$$

$$f_{cy} = f_y - \rho_{sy} f_{sy}, \tag{20}$$

$$f_{c2} = f_{c1} - v_{xy}(\tan\theta + 1/\tan\theta), \tag{21}$$

where f_x and f_y are the stresses applied to the element in the x and y directions, respectively, f_{cx} and f_{cy} are the stresses in the concrete in the x and y directions, respectively, ρ_{sx} and ρ_{sy} are the reinforcement ratios in the x and y directions, respectively, and v_{xy} is the shear stress.

After cracking, it is necessary to consider the stresses in the reinforcement at the crack location, which can be calculated as follows. Fig. 4 shows the stresses at different locations in the SFRC element.

$$f_{sxcr} = f_{sx} + (f_{c1} + f_{ci} + v_{ci}/\tan\theta)/\rho_{sx}. \tag{22}$$

The average spacing of the cracks is necessary to establish the relationship between the principal tensile strain and the crack width. In this study, the values of the average crack spacing (s_m) were obtained directly from experimental results. Accordingly, the crack width can be calculated as follows:

$$w = \varepsilon_1 s_\theta, \tag{23}$$

where s_θ is the crack spacing measured at angle θ.

$$s_\theta = \frac{1}{\left(\frac{\sin\theta}{s_{mx}} + \frac{\cos\theta}{s_{my}}\right)}. \tag{24}$$

For a given crack width, the maximum resistance to shear stress can be calculated as follows:

$$v_{ci\,max} = \frac{\sqrt{-f_c'}}{0.31 + 24w/(a + 16)}, \tag{25}$$

where a is the maximum size of the aggregate.

5 Solution Method

A solution method is proposed based on the equations presented in the previous section, as shown in the solution algorithm in Fig. 5. For this trial-and-error method, the number of iterative cycles is required for an assumed value of f_x until all conditions are fulfilled, which provides one point on the v_{xy} vs. γ_{xy} curve.
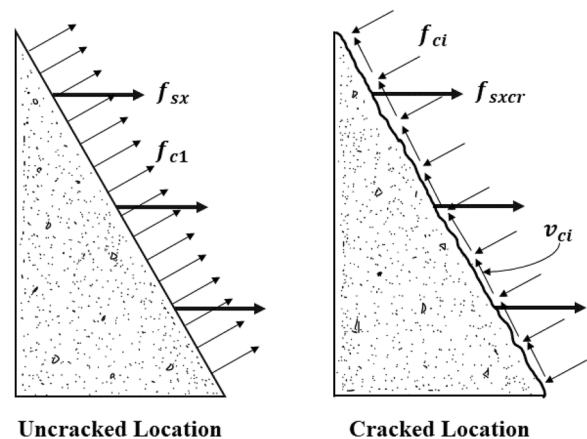
**Fig. 4** Stresses in steel and concrete at the uncracked and cracked locations
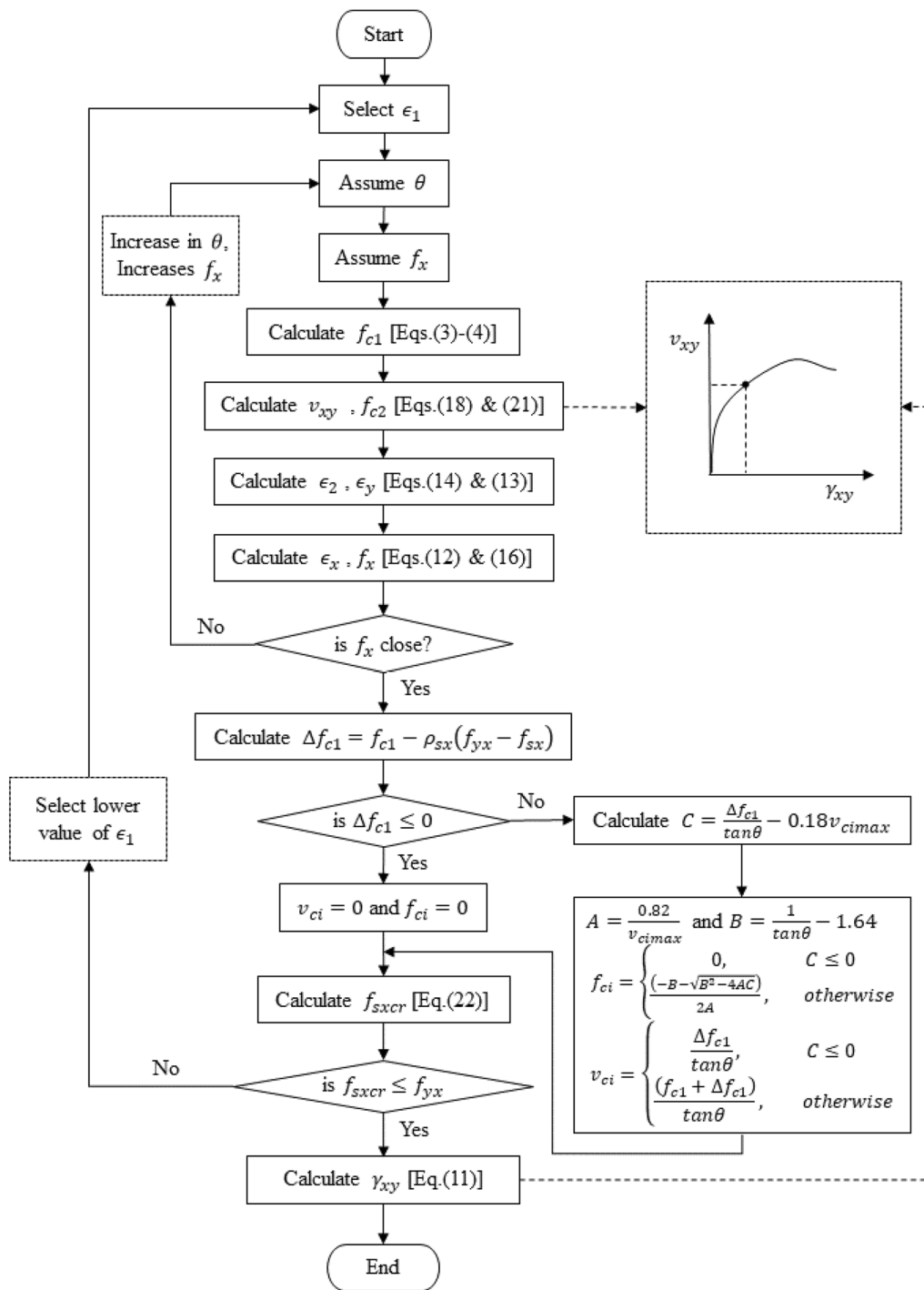
Fig. 5 Solution algorithm

At the initial stage (S), it is necessary to input all material properties, crack spacing characteristics, and properties of the fibers. The iterative procedure for obtaining the entire v_{xy} vs. γ_{xy} curve starts by assuming the values of ε_1, θ, and f_x (Steps 1 to 3). Before Step 6, it is necessary to ensure that the condition $f_{c2}/f_{c2\,max} \leq 1.0$ is satisfied; otherwise, the solution is not possible (Vecchio & Collins, 1986). If this condition is not satisfied, then another value of θ close to 45° can be assumed or a lower value of ε_1 can be selected. Consequently, this condition should

Wagh *et al. Int J Concr Struct Mater* (2023) 17:29

Page 9 of 13

Table 5 Failure patterns for the SFRC panels

| Condition	Prediction
Condition 1: $f_{c1} \leq v_{ci\,max}\left(0.18 + 0.3k^2\right)\tan\theta + \rho_{sy}\left(f_{yy} - f_{sy}\right)$, where $k = 1.64 - 1/\tan\theta$, but $k \geq 0$	Slip-on the crack
Condition 2: $f_{c2} \leq f_{c2\,max}$	Concrete shear failure
Condition 3: $f_{sxcr} \leq f_{yx}$	Yielding the reinforcement
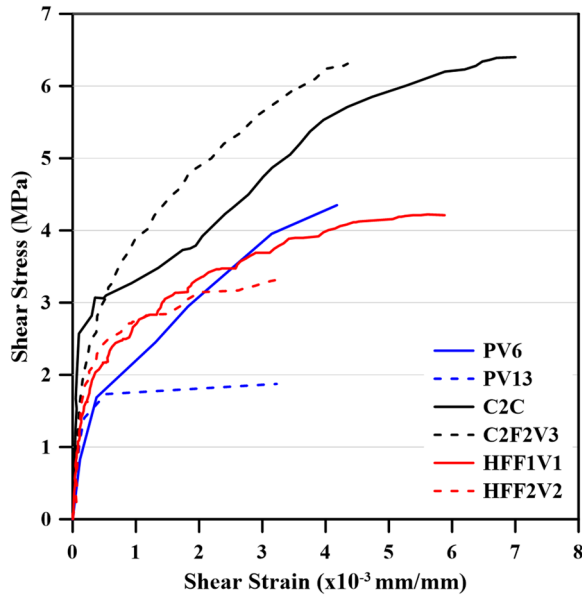
Fig. 6 Shear stress–strain response

be satisfied along with the three decision-making steps in the solution algorithm.

Compared with the upper half section, the lower half section of the solution algorithm is more complex. Minor modifications need to be made in the original MCFT in the calculation of Δf_{c1} to better characterize the behavior of SFRC with reinforcement in the longitudinal direction only. For each load stage, the computation of v_{ci} and f_{ci} may follow different routes, as indicated in the algorithm. It should also be noted that the calculated value of f_{sxcr} increases with an increase in the value of f_x. By calculating a series of f_x values and repeating Steps 1 to 11, the complete v_{xy} vs. γ_{xy} curve can be obtained.

The guidelines established by Vecchio and Collins (1986) were adopted to determine the failure pattern. The failure pattern can be determined by satisfying any of the conditions at the failure stage in Table 5. These conditions can be applied either individually or in combination with other conditions.
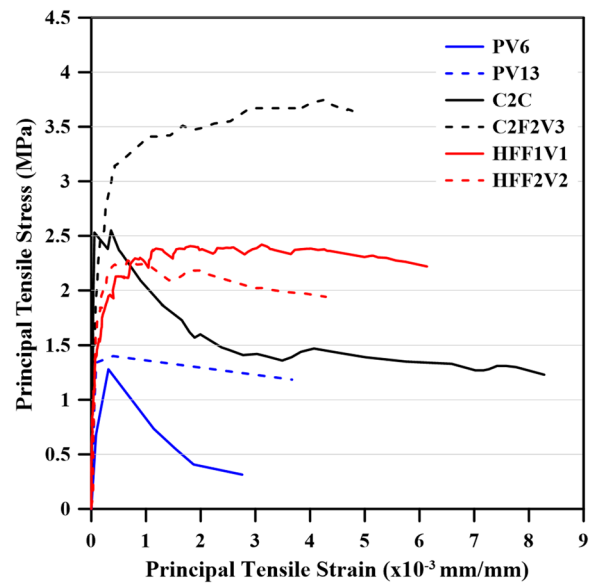

Fig. 7 Principal tensile stress–strain response

Table 6 Summary of the panel test results

Panel	Concrete		Experimental observations	
	$\varepsilon'_c\,(\times 10^{-3})$	f'_c (MPa)	v_{cr} (MPa)	v_u (MPa)
C2C	2.703	90.5	2.57	6.40
PV6	2.5	29.8	2.00	4.55
PV13	2.7	18.2	1.73	2.01
C2F2V3	2.224	76.5	1.59	6.31
HFF1V1	2.708	35	1.63	4.22
HFF2V2	2.853	21	1.90	3.31

6 Discussion of Experimental Results

Figs. 6 and 7 show the shear and tension responses of the panels, respectively. Fig. 6 shows the linear shear stress–shear strain response of the panel until the occurrence of the first crack. The values of the shear stress at the occurrence of the first crack (v_{cr}) and ultimate shear strength (v_u) are listed in Table 6. Panels PV13 and C2F2V3 achieved maximum shear stresses of 44.18% and 98.59%, respectively, compared with those of control panels PV6 and C2C, respectively. It can be observed from Fig. 6 that SFRC panel C2F2V3 with RC65/35-BN fibers achieved a shear strength approximately equal to that of control panel C2C. Similar observations can also be drawn for the panels HFF2V2 and PV13 without transverse reinforcement; with only 0.75% addition of fibers indicated an improved shear strength by 39%. This is because the addition of fibers significantly increases shear strength (Kwak et al., 2002; Narayanan & Darwish, 1987). RC panel PV13

Wagh *et al. Int J Concr Struct Mater* (2023) 17:29

Page 10 of 13

without longitudinal reinforcement achieved less than half the shear strength of control panel PV6. It can also be observed that SFRC panels HFF1V1 and HFF2V2 can achieve a shear stress of at least 73% compared with that of control panel PV6. The shear resistance exhibited by panel HFF2V2 is less than that of panel HFF1V1 because the equivalent shear resistance cannot be achieved at a low fiber content (Susetyo et al., 2011). Despite this, the response exhibited by panel HFF2V2 is satisfactory when it is considered that transverse reinforcement was not provided. Fiber-type RC80/30BP achieved the highest shear stress value because of its high tensile strength, as represented by the response of panel HFF1V1 in Fig. 8,
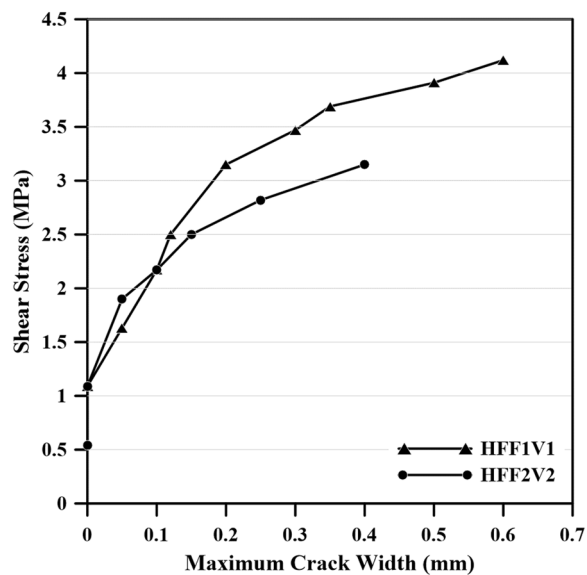
Fig. 8 Propagation of cracks in panels HFF1V1 and HFF2V2

with superior crack control characteristics compared with that of panel HFF2V2. This observation agrees with the results reported by Susetyo et. al. (2011); the compressive strength of concrete does not significantly affect the shear strength of SFRC panels, but has an effect on the type of fiber and aspect ratio. The aforementioned results indicate that the shear strength increased by 28% when the fiber content increased by a factor of two (from 0.75 to 1.5%) from panel HFF2V2 to HFF1V1. Increase in fiber aspect ratio indicates higher post-cracking deformation capabilities. Because of the lower dosage of the fibers, shear strain attained by panel HFF2V2 was 37% lower compared to panels HFF1V1 and C2F2V3.

The principal tensile stress–strain response of the panels is shown in Fig. 7. The occurrence of the first crack indicates the point of maximum principal tensile stress in the RC panels. All SFRC panels exhibited strain hardening behavior because of the presence of fibers that initiated bridging effect over the cracks and transmission of tensile stresses. However, because of the gradual deterioration of the bond between the reinforcement and concrete, all the RC panels exhibited strain softening behavior. Panel C2C exhibited brittle behavior, which is a property of high-strength concrete; moreover, the principal tensile stress decreased until failure after the occurrence of the first crack. In contrast, in specimen C2F2V3, an increase in the principal tensile stress and shear stress enhanced crack propagation control.

All the SFRC panels failed because of shear slip on the crack surface, after all the fibers were pulled out of the matrix, as well as loss of aggregate interlock. Fig. 9a, b shows the failure modes of panels HFF1V1 and HFF2V2, respectively. In panel PV13, the load suddenly decreased to 1.73 MPa as soon as the panel reached the peak load

(a)   (b)
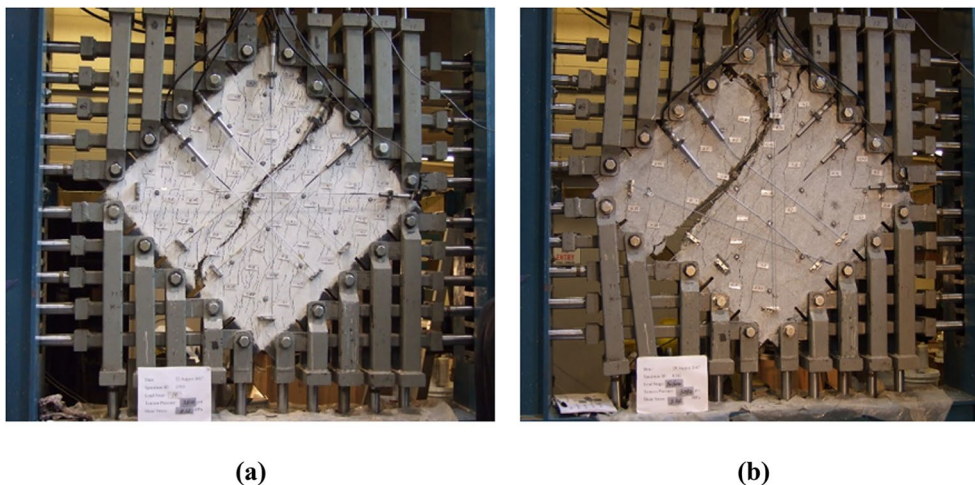
Fig. 9 Failure stage of the panel: **a** HFF1V1, **b** HFF2V2

of 2.01 MPa, and the concrete failed in shear before reinforcement yielding. In addition, RC panel PV6 failed owing to yielding of the transverse reinforcement. Sudden failure occurred in panel C2C as a result of major concrete spalling and rupture of the transverse reinforcement. At the stage of failure, plastic deformation of steel fibers was observed along the cracked surface in panels HFF1V1 and HFF2V2.

7 Verification of the Model

The proposed analytical model was used to predict the shear stress–strain response of the SFRC panel specimens to evaluate its accuracy. The values of the ultimate shear strength predicted using the proposed analytical procedure (v_{umodel}) and the experimental results (v_{uexp}) are presented in Additional file 1. The shear strength obtained using the proposed model was compared with experimental results to verify its accuracy. The dataset for 30 SFRC panels were compiled as presented in Additional file 1, of which 18 panels were used for monotonic loading, whereas the other 12 panels were used for reversed cyclic loading (Carnovale & Vecchio, 2014; Chasioti & Vecchio, 2017; Luo & Vecchio, 2016; Susetyo et al., 2011). Variations in the type of steel fibers used can be observed. Furthermore, the prediction results obtained using the proposed model for the two panels containing MAC matrix fibers (DC-P3 and DC-P5) are also presented in the bottom two rows of Additional file 1.

The results calculated from the proposed analysis procedure are plotted against the experimental results in Fig. 10a, b. The coefficient of variation (CoV) values for

monotonic and reversed cyclic loading conditions is 15.41% and 22.34%, respectively. Reversed cyclic loading conditions significantly affects the fibers bridging over the cracks and negatively affects the SFRC response (Carnovale & Vecchio, 2014; Luo & Vecchio, 2016). It is evident from CoV that shear strength prediction for monotonic loading condition is in close agreement with the experimental results compared with that of reversed cyclic loading condition. In other words, the method presented in this paper is suitable for monotonic loading condition only and does not consider the effects of reversed cyclic loading conditions. In situations where shear strength is a principal concern, the application of the proposed analysis procedure for reversed cyclic loading condition is not advisable at present.

Fig. 11 shows plots of the shear stress–strain response predicted for panels HFF1V1 and HFF2V2 using the proposed analysis procedure. The analysis results are in good agreement with experimental results for panel HFF2V2, as shown in Fig. 11b; however, minor deviations can be observed in the predicted response for panel HFF1V1, as shown in Fig. 11a. This anomaly is due to the sensitivity of the tension model (Eq. 8) and does not affect the analysis method presented. The calculated α, λ, and τ_{eq} values from the uniaxial tension test and fiber pull-out test affect the sensitivity of the model. Contrastingly, the calculated value of E_{c} (Eq. 7) does not affect the analysis response. Results from uniaxial tension tests may be easily affected by the distribution of aggregates, improper mixing, orientation and distribution of fibers in three-dimensional (3D) space, and the experimental process (Liao et al., 2020; Naaman & Shah, 2022; Susetyo, 2009).
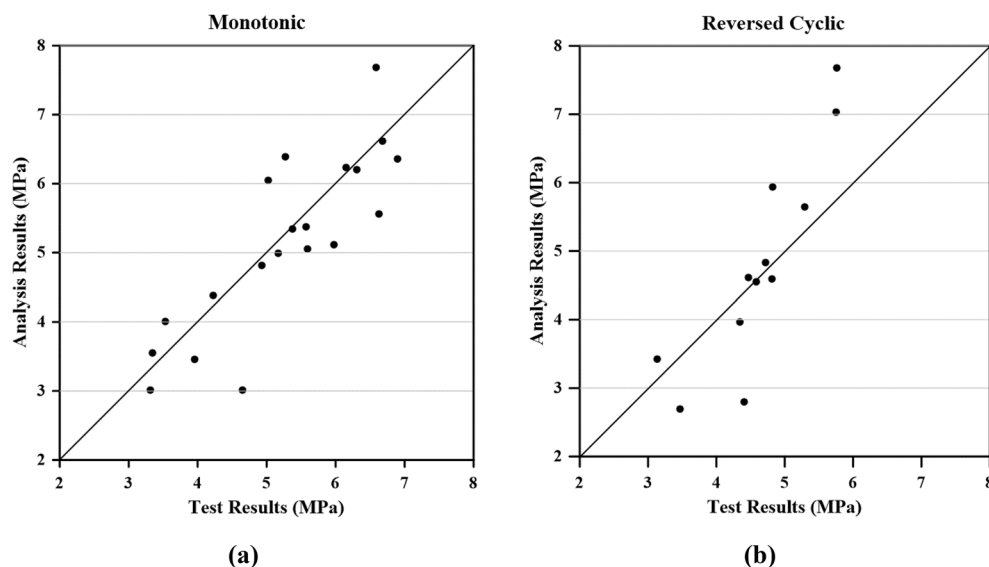
Fig. 10 Shear stress calculated using the proposed analysis procedure and the test results: **a** monotonic, **b** reversed cyclic
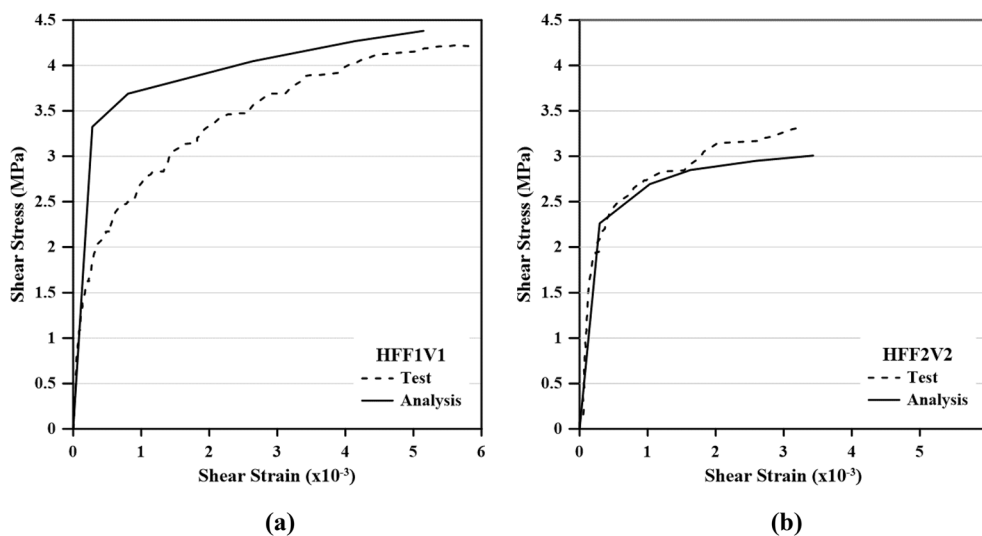
Fig. 11 Comparison of the shear stress–strain response from test and analysis: **a** HFF1V1; **b** HFF2V2

Table 7 Predicted failure patterns for the panels tested in this study

Specimen ID	Applicable conditions	Failure pattern
HFF1V1	Condition 1 and Condition 2	Shear slip
HFF2V2	Condition 1 and Condition 2	Shear slip

According to the conditions presented in Table 5, the failure pattern for both panels tested in this study can be categorized as shear–slip failure after satisfying the first two conditions listed in Table 7.

At present MCFT is being used in advanced research areas, such as fire analysis, fatigue analysis, and dynamic analysis for blast and impact loads (Sadeghian & Vecchio, 2018). Also, the use of SFRC is increasing to fix the practical engineering complications. To take the complete advantage of strain hardening properties of SFRC in structural application, the proposed study based on MCFT can be useful for researchers and structural engineers for developing computer programs to predict the shear strength.

8 Conclusion

In this study, the experimental results for three normal concrete panels and three SFRC panels were analyzed. The applicability of MCFT was evaluated to accurately determine the shear response of the SFRC panel. The main results and conclusions are summarized as follows.

1. The presence of fiber stimulates bridging effect over the cracks, and all the HF-SHSFRC panel specimens exhibited good performance in terms of shear and tension compared with conventionally reinforced concrete panels because of the strain hardening behavior. The type of fiber used also affects the strength of the concrete.

2. The proposed analysis procedure enhanced the suitability of MCFT for predicting the shear stress–strain response of SFRC panels by incorporating the effect of strain hardening due to the presence of fibers. The values of α, λ, and τ_{eq} obtained from the tension model can affect the sensitivity of the response.

3. The proposed analysis procedure was validated by comparing the result with experimental results from 30 SFRC panels. The solution method presented in this paper accurately predicted the shear strength as well as the failure pattern.

Supplementary Information

The online version contains supplementary material available at https://doi.org/10.1186/s40069-023-00586-4.

Additional file 1. Database of SFRC panel shear tests.

Wagh *et al. Int J Concr Struct Mater*   (2023) 17:29

Page 13 of 13

Authors' information
Suyash K. Wagh is a Ph.D. Candidate in the Department of Civil Engineering at the National Taiwan University. His research interests include shear behavior of reinforced concrete and analysis of fiber-reinforced concrete.
Agie Vianthi is a former graduate student in Structural Engineering Division at the Department of Civil Engineering, National Taiwan University.
Wen-Cheng Liao is a Professor in the Department of Civil Engineering at the National Taiwan University. He received his Ph.D. from the University of Michigan, Ann Arbor, MI, USA. His research interests include mechanics of materials, prediction of creep and shrinkage of concrete, and analysis and design of concrete structures, particularly using high performance fiber-reinforced concrete.

Availability of data and materials
Detailed calculations based on the proposed analytical procedure are available from the corresponding author on reasonable request.

Declarations

Competing interests
The authors declare that they have no competing interests.

References
ACI Committee 363. (2005). *High-strength concrete (ACI 363R)*. American Concrete Institute.
Ashour, S. A., Hasanain, G. S., & Wafa, F. F. (1992). Shear behavior of high-strength fiber reinforced concrete beams. *ACI Structural Journal, 89*(2), 176–184.
Carnovale, D., & Vecchio, F. J. (2014). Effect of fiber material and loading history on shear behavior of fiber-reinforced concrete. *ACI Structural Journal, 111*(5), 1235–1244. https://doi.org/10.14359/51686809
Chao, S. H., Liao, W. C., Wongtanakitcharoen, T., & Naaman, A. (2007). Large scale tensile tests of high performance fiber reinforced cement composites. In *Fifth international RILEM workshop on high performance fiber reinforced cement composites (HPFRCC5)*.
Chasioti, S. G., & Vecchio, F. J. (2017). Shear behavior and crack control characteristics of hybrid steel fiber-reinforced concrete panels. *ACI Structural Journal, 114*(1), 209–220. https://doi.org/10.14359/51689164
Collins, M. P. (1978). Towards a rational theory for RC members in shear. *Journal of the Structural Division, 104*(4), 649–666. https://doi.org/10.1061/JSDEAG.0004900
Evans, R., & Marathe, M. (1968). Microcracking and stress–strain curves for concrete in tension. *Materials and Structures, 1*(1), 61–64.
Kwak, Y., Eberhard, M. O., Kim, W., & Kim, J. (2002). Shear strength of steel fiber-reinforced concrete beams without stirrups. *ACI Structural Journal, 99*(4), 530–538.
Lee, S., Cho, J., & Vecchio, F. J. (2016). Analysis of steel fiber-reinforced concrete elements subjected to shear. *ACI Structural Journal, 113*(2), 275–286. https://doi.org/10.14359/51688474
Lee, S. C., Cho, J. Y., & Vecchio, F. J. (2011). Diverse embedment model for steel fiber-reinforced concrete in tension: Model development. *ACI Materials Journal, 110*(4), 516–525. https://doi.org/10.14359/51685787
Liao, W. C., Chao, S. H., Park, S. Y., & Naaman, A. E. (2006). *Self-consolidating high performance fiber reinforced concrete (SCHPFRC)—Preliminary investigation UMCEE 06-02*.
Liao, W. C., Chen, P. S., Hung, C. W., & Wagh, S. K. (2020). An innovative test method for tensile strength of concrete by applying the strut-and-tie methodology. *Materials, 13*(12), 1–20. https://doi.org/10.3390/ma13122776
Liao, W. C., Perceka, W., & Liu, E. J. (2015). Compressive stress–strain relationship of high strength steel fiber reinforced concrete. *Journal of Advanced Concrete Technology, 13*(8), 379–392. https://doi.org/10.3151/jact.13.379
Liao, W. C., Perceka, W., & Yu, L. C. (2017). Systematic mix procedures for highly flowable-strain hardening fiber reinforced concrete (HF-SHFRC) by using tensile strain hardening responses as performance criteria. *Science of Advanced Materials, 9*(7), 1157–1168. https://doi.org/10.1166/sam.2017.3097
Liao, W. C., & Su, W. R. (2018). Implementation of highly-flowable strain hardening fiber reinforced concrete in new RC beam-column joints. *MATEC Web of Conferences*. https://doi.org/10.1051/matecconf/201814701003
Luo, J. W., & Vecchio, F. J. (2016). Behavior of steel fiber-reinforced concrete under reversed cyclic shear. *ACI Structural Journal, 113*(1), 75–84. https://doi.org/10.14359/51687940
Mansur, M. A., Ong, K. C. G., & Paramasivam, P. (1986). Shear strength of fibrous concrete beams without stirrups. *Journal of Structural Engineering, 112*(9), 2066–2079.
Mitchell, D., & Collins, M. P. (1974). Diagonal compression field theory—A rational model for structural concrete in pure torsion. *ACI Journal, 71*(8), 396–408.
Naaman, A. E. (1972). *A statistical theory of strength for fiber reinforced concrete*. Massachusetts Institute of Technology.
Naaman, A. E., & Shah, S. P. (2022). Strain capacity of strain-hardening ultra-high-performance concrete with steel fibers. *ACI Materials Journal, 119*(2), 171–180. https://doi.org/10.14359/51734357
Narayanan, R., & Darwish, I. Y. S. (1987). Use of steel fibers as shear reinforcement. *ACI Structural Journal, 84*(3), 216–227.
Noghabai, K. (2000). Beams of fibrous concrete in shear and bending: Experiment and model. *Journal of Structural Engineering, 126*(2), 243–251.
Parra-montesinos, G. J. (2006). Shear strength of beams with deformed steel fibers evaluating an alternative to minimum transverse reinforcement. *Concrete International, 28*(11), 57–67.
Sadeghian, V., & Vecchio, F. (2018). *SP-328-3 the modified compression field theory: Then and now*. ACI Special Publication SP-328.
Susetyo, J. (2009). *Fibre reinforcement for shrinkage crack control in prestressed*. University of Toronto.
Susetyo, J., Gauvreau, P., & Vecchio, F. J. (2011). Effectiveness of steel fiber as minimum shear reinforcement. *ACI Structural Journal, 108*(4), 488–496.
Susetyo, J., Gauvreau, P., & Vecchio, F. J. (2013). Steel fiber-reinforced concrete panels in shear: Analysis and modeling. *ACI Structural Journal, 110*(2), 285–295. https://doi.org/10.14359/51684408
Vecchio, F. (1982). *The response of reinforced concrete to in-plane shear and normal stresses*. University of Toronto.
Vecchio, F. J. (2000). Disturbed stress field model for reinforced concrete: Formulation. *Journal of Structural Engineering, 126*(9), 1070–1077. https://doi.org/10.1061/(asce)0733-9445(2000)126:9(1070)
Vecchio, F. J., & Collins, M. P. (1986). The modified compression-field theory for reinforced concrete elements subjected to shear. *ACI Journal, 83*(22), 219–231.
Voo, J. Y. L., & Foster, S. J. (2003). Variable engagement model for fibre reinforced concrete in tension. In *Uniciv report no. R-420, School of Civil and Environmental Engineering, University of New South Wales*.

Publisher's Note
Springer Nature remains neutral with regard to jurisdictional claims in published maps and institutional affiliations.